VOL. 10, NO. 12, JULY 2015 ISSN 1819-6608
ARPN Journal of Engineering and Applied Sciences

www.arpnjournals.com

CHARACTERIZATION OF THE NATURALLY FRACTURED RESERVOIR PARAMETERS IN INFINITE-CONDUCTIVITY HYDRAULICALLY-FRACTURED VERTICAL WELLS BY TRANSIENT PRESSURE ANALYSIS

Freddy Humberto Escobar[1], Yu Long Zhao[2] and Mashhad Fahes[3]
[1]Universidad Surcolombiana/CENIGAA, Avenida Pastrana - Cra 1, Neiva, Huila, Colombia
[2]State Key Laboratory of Oil and Gas Reservoir Geology and Exploitation, Southwest Petroleum University, Xindu Street, Xindu district, Chendu, Sichuan, P. R. China
[3]The University of Oklahoma, Mewbourne School of Petroleum and Geological Engineering, E. Boyd St. SEC Rm, Norman, Ok, USA
E-Mail: fescobar@usco.edu.co

ABSTRACT

It has become common to hydraulically fracture a naturally fractured formation to increase the well's production potential. Since the mass transfer between fractured network and hydraulic fracture is much higher than that from matrix to fractures, the hydraulic fracture-fracture network interporosity flow parameter is much higher that that of matrix-fracture network. As a result, the transition period behavior from naturally fractured to homogeneous takes place before radial flow regime during the early bilinear, linear or elliptical (birradial) flow regimes. The purpose of this paper is to provide expressions by both conventional analysis and *TDS* technique for characterizing the naturally fractured parameters when the transition period interrupts the response of an infinite-conductivity fracture. The developed expressions for both methodologies were satisfactorily tested with simulated examples.

Keywords: pressure transient analysis, interporosity flow parameter, *TDS* technique, elliptical flow, naturally fractured reservoirs.

1. INTRODUCTION

Even wells in naturally fractured formations are being subjected to hydraulic fracturing since the bulk permeability is low and well productivity is not as high as expected. Typical such cases have been seen in some wells of the Orinoco basin foothill in Colombia where the wells were fractured just after being drilled.

Tiab (1994) was the first to identify the elliptical flow regime in pressure test data of infinite-conductivity hydraulically fractured vertical wells. He called it "*birradial flow*", provided the governing pressure and pressure derivative equations and implemented the *TDS* technique for its characterization. This flow regime can also be seen in horizontal wells before the late radial flow regime shows up and is due mainly to horizontal anisotropy. The last model for the elliptical flow in horizontal wells was presented by Martinez, Escobar and Bonilla (2012).

The original pressure governing model for elliptical flow introduced by Tiab (1994) involves the drainage area, which may affect the calculations if the pressure test is too short for the development of the late pseudosteady-state period. An experienced user of the *TDS* technique may deal with that problem using the point of intersection between the radial flow and the birradial flow regime lines, Tiab (1994). However, to overcome this problem, Escobar, Bonilla and Ghisays-Ruiz (2014) formulated a new elliptical/birradial flow model for vertical wells in either fractured or unfractured formations.

Although Tiab's model, Tiab (1994), works perfectly, it requires the knowledge of well-drainage area for estimating the half-fracture length. However, sometimes this condition cannot be met because the pressure test needs to be run long enough for the development of the late time pseudosteady-state period for the determination of the drainage area. The new model presented by Escobar *et al*. (2014) excludes the reservoir drainage area and slightly modifies Tiab's model, Tiab (1994), to account for naturally-fractured double-porosity systems.

Tiab and Bettam (2007) presented a practical interpretation of the pressure behavior of a finite-conductivity hydraulically fractured vertical well located in a naturally fractured reservoir. The interpretation is based on analytical equations derived to determine permeability, fracture storage capacity ratio, interporosity flow coefficient, skin and wellbore storage from the pressure derivative plot without using type-curve matching technique. In other words, they implemented the *TDS* technique, Tiab (1993), for such systems. Part of the work presented by Escobar, Martinez and Montealegre (2009) was focused on the implementation of conventional analysis for the work presented by Tiab and Bettam (2007).

In their work, Tiab and Bettam (2007) developed expressions for bilinear and linear flow regimes but excluded the presence of the elliptical or birradial flow regime. Thereafter, this work constitutes an extension of

VOL. 10, NO. 12, JULY 2015 ISSN 1819-6608
ARPN Journal of Engineering and Applied Sciences

www.arpnjournals.com

the research of Tiab and Bettam (2007) for infinite-conductivity fractures where early birradial flow is seen. This implementation was satisfactorily tested with synthetic examples.

2. MATHEMATICAL FORMULATION

2.1. Governing equation

The dimensionless pressure behavior in the Laplace domain for a hydraulically fractured well in double-porosity reservoirs was introduced by Ozkan and Raghavan (1988):

$$\bar{P}_D(s) = \frac{1}{2s\sqrt{sf(s)}} \int_0^{s\sqrt{sf(s)}[1\pm 0.732)} K_0(\alpha)d\alpha \tag{1}$$

For a pseudosteady-state matrix flow model, the function of storage capacity and interporosity flow parameter is given by:

$$f(s) = \omega + \frac{(1-\omega)\lambda_f}{(1-\omega)s + \lambda_f} \tag{2}$$

Escobar *et al.* (2014) provided the following pressure and pressure derivative governing equations for elliptical flow regime:

$$P_D = \frac{25}{9}\left(\frac{\pi t_{Dxf}}{26\xi}\right)^{0.36} \tag{3}$$

$$t_D * P_D' = \left(\frac{\pi t_{Dxf}}{26\xi}\right)^{0.36} \tag{4}$$

When ξ = 1, Equations (3) and (4) account for homogeneous reservoirs. For the case of naturally-fractured formations, ξ = ω, which is the dimensionless storativity coefficient. Consequently, for the purpose of this work, ξ will be replaced by the storativity ratio.

2.2. Dimensionless quantities

The dimensionless time, based on half-fracture length, is given below:

$$t_{Dxf} = \frac{0.000263kt}{\phi\mu c_t x_f^2} \tag{5}$$

The dimensionless pressure and pressure derivative parameters for oil reservoirs are given by:

$$P_D = \frac{kh\Delta P}{141.2q\mu B} \tag{6}$$

$$t_D * P_D' = \frac{kh(t*\Delta P')}{141.2q\mu B} \tag{7}$$

Finally, the dimensionless fracture conductivity introduced by Cinco-Ley, Samaniego and Dominguez (1976) is defined as:

$$C_{fD} = \frac{k_f w_f}{k\,x_f} \tag{8}$$

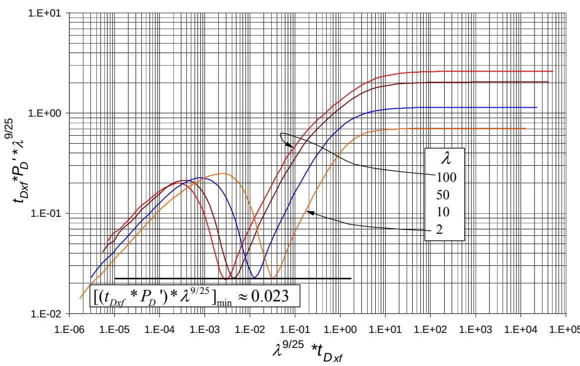

Figure-1. Effect of the interporosity flow parameter on the pressure and pressure derivative during the elliptical flow regime, $\omega = 0.01$.

2.3. *TDS* technique

By plugging the dimensionless parameters in Equations (3) and (4) and solving for the half-fracture length, we obtain:

$$x_f = 22.5632\left(\frac{qB}{h\Delta P_{BR1}}\right)^{1.3889}\sqrt{\frac{1}{\omega\phi c_t}\left(\frac{\mu}{k}\right)^{1.778}} \tag{9}$$

$$x_f = 5.4595\left(\frac{qB}{h(t*\Delta P')_{BR1}}\right)^{1.3889}\sqrt{\frac{1}{\omega\phi c_t}\left(\frac{\mu}{k}\right)^{1.778}} \tag{10}$$

Figures-1 through 4 were generated using the analytical solution provided by Ozkan and Raghavan (1988), Equation (1), which considers flow between hydraulic fracture and fracture network.

As seen in Figure-1, once the transition period vanishes, the reservoir behaves as if it were homogeneous. In this case, Equations (9) and (10) become:

VOL. 10, NO. 12, JULY 2015 ISSN 1819-6608
ARPN Journal of Engineering and Applied Sciences

www.arpnjournals.com

$$x_f = 22.5632\left(\frac{qB}{h\Delta P_{2BR1}}\right)^{1.3889}\sqrt{\frac{1}{\phi c_t}\left(\frac{\mu}{k}\right)^{1.778}} \tag{11}$$

$$x_f = 5.4595\left(\frac{qB}{h(t*\Delta P')_{2BR1}}\right)^{1.3889}\sqrt{\frac{1}{\phi c_t}\left(\frac{\mu}{k}\right)^{1.778}} \tag{12}$$

Where $2BR1$ corresponds to the straight line drawn on the second elliptical flow regime which occurs after the transition period. However, before the transition period either elliptical flow or linear flow may take place. If linear flow occurs at early time, then Equations (9) and (10) must be replaced by these two expressions developed by Tiab and Bettam (2007);

$$x_f = 4.064\left(\frac{qB}{\Delta P_{L1} h\sqrt{\omega}}\right)\sqrt{\frac{\mu}{(\phi c_t)_t k}} \tag{13}$$

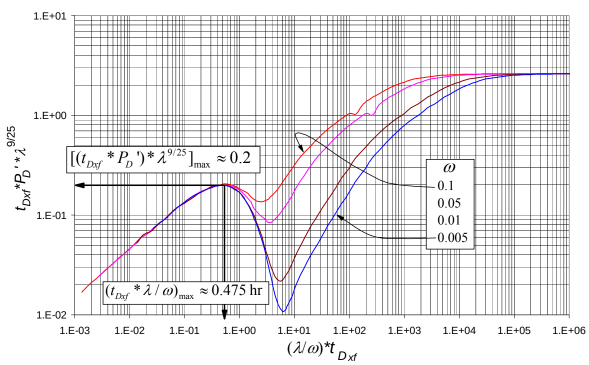

Figure-2. Correlation of the maximum and minimum pressure derivative coordinates during elliptical flow period, λ_f = 100.

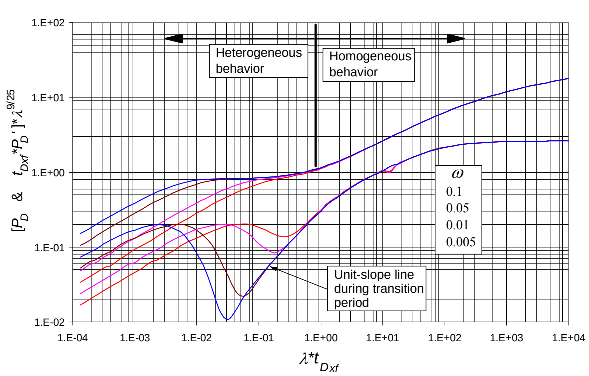

Figure-3. Effect of the storativity ratio on the pressure and pressure derivative during the elliptical flow regime, λ_f = 100.

$$x_f = 2.032\left(\frac{qB}{(t*\Delta P')_{L1} h\sqrt{\omega}}\right)\sqrt{\frac{\mu}{(\phi c_t)k}} \tag{14}$$

Fracture conductivity can be found using an expression presented by Tiab (2003);

$$k_f w_f = \frac{3.31739k}{\frac{e^s}{r_w}-\frac{1.92173}{x_f}} \tag{15}$$

It is observed in Figure-1 that the minimum point of the pressure derivative times the interporosity flow parameter to the power 0.36 is a constant:

$$(t_{Dxf} * P_D')_{\min}\,\lambda_f^{9/25} \approx 0.023 \tag{16}$$

The following expression to determine the interporosity flow parameter is obtained once Equation (7) is substituted in Equation (16):

$$\lambda_f \approx 26.364\left[\frac{q\mu B}{kh(t*\Delta P')_{\min}}\right]^{25/9} \tag{17}$$

Figure-2 contains a log-log plot of pressure and pressure derivative both multiplied by the interporosity flow parameter raised to the power 9/25 (or 0.36) versus dimensionless time multiplied by interporosity flow parameter and divided by the storativity ratio. During the early heterogeneous behavior, all curves unify no matter the values of storativity ratio. A maximum point is displayed before the transition period which coordinates are given by:

$$[(t_{Dxf} * P_D')\ \lambda_f^{9/25}]_{\max} \approx 0.2 \tag{18}$$

$$\left(\frac{t_{Dxf}\cdot\lambda_f}{\omega}\right)_{\max} \approx 0.475 \tag{19}$$

Once Equation (7) is substituted into Equation (18), we obtain:

$$\lambda_f \approx 10719.63\left[\frac{q\mu B}{kh(t*\Delta P')_{\max}}\right]^{25/9} \tag{20}$$

Substituting Equation (5) into Equation (19) yields two expressions to find either interporosity flow parameter or storativity ratio one as a function of the other so;

VOL. 10, NO. 12, JULY 2015 ISSN 1819-6608
ARPN Journal of Engineering and Applied Sciences

$$\omega = \frac{\lambda_f k t_{\max}}{1801.29 \phi \mu c_t x_f^2} \tag{21}$$

$$\lambda_f = \frac{1801.29 \omega \phi \mu c_t x_f^2}{k t_{\max}} \tag{22}$$

Figure-3 was prepared to unify the unit-slope line showing up during the transition period. Such straight line was fitted to:

$$(t_{Dxf} * P_D') = 0.3862 t_{Dxf} \lambda_f^{16/25} \tag{23}$$

After substituting the dimensionless parameter and solving for the interporosity flow parameter, it yields:

$$\lambda_f = 755.94 \left(\frac{\phi c_t x_f^2 h (t*\Delta P')_{us}}{qBt_{us}} \right)^{25/16} \tag{24}$$

Equation (24) works using the coordinates of any point along the unit-slope line. During radial flow regime, the value of the dimensionless pressure derivative is one half. Equating this value to Equation (23) and solving for the interporosity flow parameter, we get:

$$\lambda_f = 585120.28 \left(\frac{\phi \mu c_t x_f^2}{k t_{usi}} \right)^{25/16} \tag{25}$$

Where t_{usi} is the intersection point of the unit-slope line and the radial flow regime.

From observation of the minimum point in Figure-2, an expression with a correlation coefficient of 0.999 was obtained:

$$\omega = 0.0002 \left(\frac{t_{\min}}{t_{\max}} \right)^2 - 0.0155 \left(\frac{t_{\min}}{t_{\max}} \right) + 0.2487 \tag{26}$$

Dividing Equation (10) by Equation (12) and solving for the storativity ratio, we get:

$$\omega = \left[\frac{(t*\Delta P')_{2BR1}}{(t*\Delta P')_{BR1}} \right]^{2.7778} \tag{27}$$

Equation (27) is valid whenever birradial/elliptical flow exists at both side of the transition period. However, in infinite-conductivity fracture, it is possible that the linear flow occurs at early time, and then is interrupted by the transition period, followed by the elliptical or birradial flow. In such cases, dividing Equation (14) by Equation (12) leads to:

$$\omega = 0.13853 \left(\frac{h}{qB} \right)^{0.778} \left[\frac{(t*\Delta P')_{2BR1}^{1.3889}}{(t*\Delta P')_{L1}} \right]^2 \left(\frac{k}{\mu} \right)^{0.778} \tag{28}$$

The point of intersection between the early birradial line, Equation (4), and the unit-slope line during the transition period, Equation (23), leads to the following expression:

$$\omega = \frac{1}{1456.69} \left(\frac{k \lambda_f t_{usBRi}}{\phi \mu c_t x_f^2} \right)^{9/16} \tag{29}$$

Tiab and Bettam (2007) introduced the governing pressure derivative equation for early linear flow:

$$t_D * P_D' = \frac{1}{2} \sqrt{\frac{t_{Dxf}}{\omega}} \tag{30}$$

Which, in combination with Equation (23), leads to:

$$\omega = \frac{6356.314 \phi \mu c_t x_f^2}{k \lambda_f^{32/25} t_{usLi}} \tag{31}$$

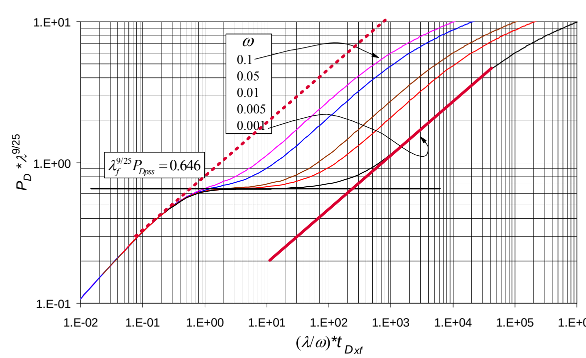

Figure-4. Dimensionless pressure times the interporosity flow parameter to the power 0.36 versus dimensionless time multiplied by λ/ω, $\lambda_f = 100$.

2.4. Conventional analysis

As seen in Figure-4, there is a point in which the dimensionless pressure converges to a value during the transition period. From there we can read that:

$$\lambda_f^{9/25} P_{Dpss} = 0.833 \tag{32}$$

VOL. 10, NO. 12, JULY 2015 ISSN 1819-6608
ARPN Journal of Engineering and Applied Sciences

www.arpnjournals.com

Substituting Equation (32) in and solving for the interporosity flow parameter yields:

$$\lambda_f = 564069.34\left[\frac{q\mu B}{kh\Delta P_{pss}}\right]^{25/9} \tag{33}$$

As seen in Figure-4, once the transition period vanishes a line with slope of 0.4 is developed. Draw such line and draw a parallel line throughout the points just before the development of the transition period. Read two points in both lines at the same time value and take its ratio, which is used in the following fitting equation that has a correlation coefficient of 0.999. The storativity ratio is found from such separation:

$$\omega = 0.3625\,\mathrm{e}^{-0.9877\frac{\Delta P_{high}}{\Delta P_{low}}} \tag{34}$$

3. SYNTHETIC EXAMPLES

3.1. Synthetic example 1

Figure-5 reports simulated pressure drop versus time data obtained with the information given on the second column of Table-1. It is required to find the naturally-fractured reservoir parameters.

Solution by Conventional Analysis

In Figure-5 a horizontal line was drawn going through the transition points. The following value of pressure drop was read:

$\Delta P_{pss} = 3.2$ psi

Using the above value in Equation (33), it yields:

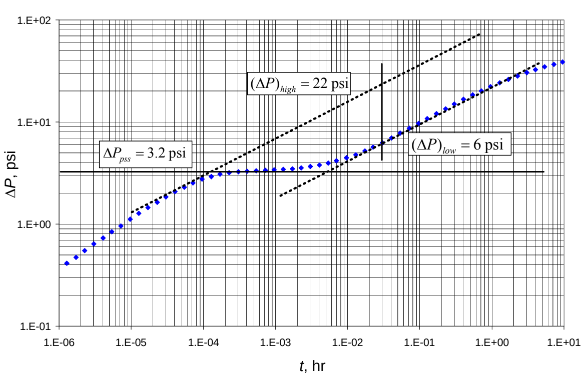

Figure-5. Pressure drop versus time log-log plot for example 1.

Table-1. Input data for examples.

	Examples	
Parameter	**1**	**2**
k, md	5	1
h, ft	100	20
ϕ, %	5	10
B, rb/STB	1.2	1.1
μ, cp	1.5	3
c_t, 1/psi	1×10^{-4}	1×10^{-4}
q, BPD	30	50
x_f, ft	10	30
λ_f	50	100
ω	0.01	0.005

$$\lambda_f = 564069.34\left[\frac{(50)(1.5)(1.2)}{(5)(100)(3.2)}\right]^{25/9} = 46.05$$

Then, a 0.4-slope line is drawn after the transition period. Another parallel line goes just after the initiation of the transition period so the amplitude can be estimated. Two pressure drop values are read at the same time from both straight lines, so:

$\Delta P_{high} = 22$ psi
$\Delta P_{low} = 6$ psi

Equation (34) will lead to the estimation of the storativity ratio:

$$\omega = 0.3625\,\mathrm{e}^{-0.9877\frac{22}{6}} = 0.0097 \approx 0.01$$

The half-fracture length is found from the slope of a Cartesian plot (m_L= 360.8 psi/hr$^{0.5}$) of pressure versus the square root of time, Figure-7, using Equation (A.7):

$$x_f = 4.064\left(\frac{30(1.2)}{(100)(360.8)}\right)\sqrt{\frac{1.5}{(0.05)(0.0001)(5)(0.01)}} = 9.93\text{ ft}$$

Solution by *TDS* Technique

ARPN Journal of Engineering and Applied Sciences

www.arpnjournals.com

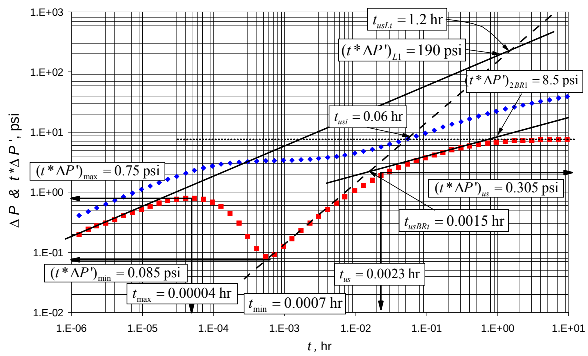

Figure-6. Pressure and pressure derivative versus time log-log plot for example 1.

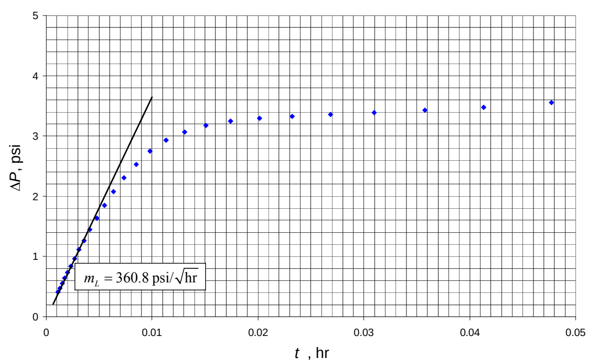

Figure-7. Cartesian plot of pressure versus the square root of time for example 1.

The following information was read from the pressure and pressure derivative log-log plot provided in Figure-6.

$t_{max} = 0.00004$ hr	$(t*\Delta P')_{2BR1} = 8.5$ psi
$(t*\Delta P')_{max} = 0.75$ psi	$(t*\Delta P')_{L1} = 190$ psi
$(t*\Delta P')_{min} = 0.085$ psi	$t_{us} = 0.0023$ hr
$(t*\Delta P')_{us} = 0.305$ psi	$t_{usi} = 0.06$ hr
$t_{usBRi} = 0.015$ hr	$t_{usLi} = 1.2$ hr
$(t*\Delta P')_{2BR1} = 8.5$ psi	$t_{min} = 0.0007$ hr

Using Equation (14);

$$x_f = 2.032\left(\frac{30(1.2)}{(190)(100)\sqrt{0.01}}\right)\sqrt{\frac{1.5}{0.05(0.0001)(5)}} = 9.43\,\text{ft}$$

The half-fracture length is also found with Equation (12);

$$x_f = 5.4595\left(\frac{30(1.2)}{100(8.5)}\right)^{1.3889}\sqrt{\frac{1}{0.05(0.0001)}\left(\frac{1.5}{5}\right)^{1.778}} = 10.37\,\text{ft}$$

The interporosity flow parameter is estimated with Equations (17), (20), (22), (24) and (25):

$$\lambda_f \approx 26.364\left[\frac{30(1.5)(1.2)}{5(100)(0.085)}\right]^{25/9} = 51.28$$

$$\lambda_f \approx 10719.63\left[\frac{30(1.5)(1.2)}{5(100)(0.75)}\right]^{25/9} = 49.24$$

$$\lambda_f = \frac{1801.29(0.1)(0.05)(1.5)(0.0001)(10^2)}{5(0.00004)} = 45.03$$

$$\lambda_f = 755.94\left(\frac{(0.05)(0.0001)(10^2)(100)(0.305)}{(30)(1.2)(0.0023)}\right)^{25/16} = 54.6$$

$$\lambda_f = 585120.28\left(\frac{(0.05)(0.0001)(10^2)}{5(0.06)}\right)^{25/16} = 50.3$$

The storativity ratio is estimated with Equations (26), (28), (29) and (31):

$$\omega = 0.0002\left(\frac{0.0007}{0.00004}\right)^2 - 0.0155\left(\frac{0.0007}{0.00004}\right) + 0.2487 = 0.039$$

$$\omega = 0.13853\left(\frac{100}{30(1.2)}\right)^{0.778}\left[\frac{(8.5)^{1.3889}}{(190)}\right]^2\left(\frac{5}{1.5}\right)^{0.778} = 0.0083$$

$$\omega = \frac{1}{1456.69}\left(\frac{5(50)(0.015)}{(0.05)(1.5)(0.0001)(10^2)}\right)^{9/16} = 0.082$$

$$\omega = \frac{6356.314(0.05)(1.5)(0.0001)(10^2)}{(5)(50^{32/25})(1.2)} = 0.005$$

3.2. Synthetic example 2

Figure-8 presents synthetic pressure drop versus time data obtained with the information given on the third column of Table-1. It is required to find the naturally-fractured reservoir parameters.

Solution by Conventional Analysis

In Figure-8 a horizontal line was drawn going through the transition points. The following value of pressure drop was read:

$\Delta P_{pss} = 184$ psi
$\Delta P_{high} = 1600$ psi
$\Delta P_{low} = 373$ psi

VOL. 10, NO. 12, JULY 2015 ISSN 1819-6608
ARPN Journal of Engineering and Applied Sciences

m_L = 2465.84 psi/hr$^{0.5}$ read from Figure-10.

Equation (33) leads to an estimation of a value 101.36 for the interporosity flow parameter and Equation (34) provides a storativity ratio of 0.00523. A half-fracture length of 35.1 ft is found with Equation (A.7)

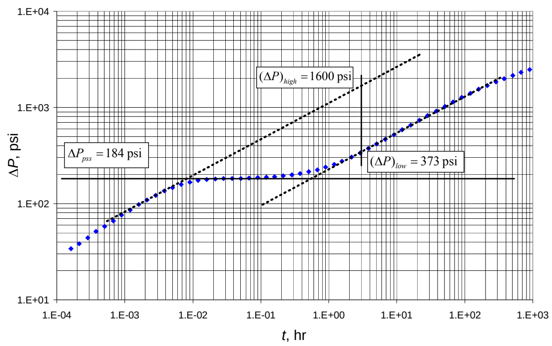

Figure-8. Pressure drop versus time log-log plot for example 1.

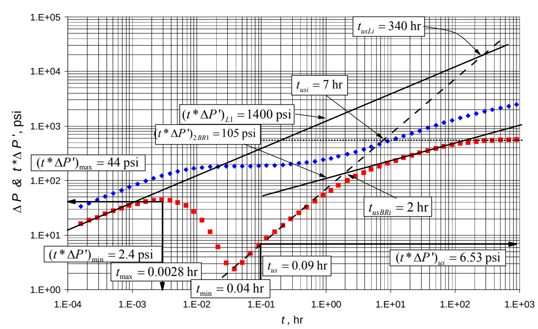

Figure-9. Pressure and pressure derivative versus time log-log plot for example 2.

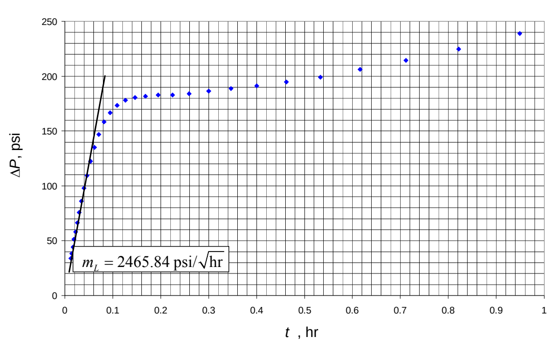

Figure-10. Cartesian plot of pressure versus the square root of time for example 2.

Solution by *TDS* Technique

The following information was read from the pressure and pressure derivative log-log plot provided in Figure-9.

t_{max} = 0.0028 hr $(t*\Delta P')_{2BR1}$=105 psi
$(t*\Delta P')_{max}$= 44 psi $(t*\Delta P')_{L1}$= 1400 psi
$(t*\Delta P')_{min}$= 2.4 psi t_{us} = 0.09 hr
t_{usBRi} = 2 hr t_{usLi} = 340 hr
$(t*\Delta P')_{us}$= 6.53 psi t_{min} = 0.04 hr

The calculations were performed in the same way as in example 1 and a summary of the results is given in Table-3.

Table-2. Results from conventional analysis.

Para-meter	Example 1	Input	Example 2	Input	Equation Number
x_f, ft	9.93	10	35.1	30	A.7
λ_f	46.05	50	101.36	100	33
ω	0.0097	0.01	0.00523	0.005	34

Table-3. Results from *TDS* technique.

Parameter	Example 1	Example 2	Equation Number
x_f, ft	10	30	**Input**
	9.43	30.91	14
	10.37	29.12	12
λ_f	50	100	**Input**
	51.28	813.9	17
	49.24	102.5	20
	45.03	28.95	22
	54.6	79.96	24
	50.3	99.03	25
ω	0.01	0.005	**Input**
	0.039	0.068	26
	0.083	0.0056	28
	0.082	0.069	29
	0.005	0.0034	31

4. COMMENTS ON THE RESULTS

The provided examples in this work demonstrate the applicability of the developed mathematical expressions. It is worth to remind that the estimation of the naturally fractured parameters is very sensitive, and as a result, deviation errors of one order of magnitude are allowed. The method provides satisfactory results especially for the interporosity flow parameter. If further

VOL. 10, NO. 12, JULY 2015 ISSN 1819-6608
ARPN Journal of Engineering and Applied Sciences

www.arpnjournals.com

accuracy is required, then, use of computer program is highly recommended. These examples were performed by hand and the values form the plots were read by eye, consequently, deviation from input values is expected.

Equations for gas flow are given in Appendix B and the equations for the estimation of half-fracture length are given in Appendix A.

CONCLUSIONS

a) New mathematical expressions for both *TDS* technique and conventional analysis were introduced and successfully tested with synthetic cases for the full characterization of pressure tests conducted in naturally-fractured reservoirs whose wells have been subjected to hydraulic fracturing.

b) For the case of the TDs technique, five expressions for the estimation of the interporosity flow parameter were developed. Four equations for the estimation of the storativity ratio were also introduced in this work.

ACKNOWLEDGEMENTS

The authors thank Universidad Surcolombiana, the University of Oklahoma and the National Science Fund for Distinguished Young Scholars of China (Grant No. 51125019) and the National Program on Key Basic Research Project (973 Program, Grant No. 2011CB201005), and the Natural Science Foundation of China (Grant No.51374181).

Nomenclature

A	Draining area, ft^2
B	Oil volume factor, rb/STB
b_x	Shortest distance from a lateral bounday to a well, ft
C_{fD}	Dimensionless fracture conductivity
c_t	Compressibility, 1/psi
h	Formation thickness, ft
k	Formation compressibility, md
k_fw_f	Fracture conductivity, md-ft
m	Slope
P	Pressure, psi
P_{wf}	Well-flowing pressure, psi
q	Oil flow rate, STB/D
q_g	Gas flow rate, MSCF/D
r_w	Wellbore radius, ft
x_f	Half-fracture lenght, ft
s	Skin factor. Laplace parameter
t	Test time, hr
T	Reservoir temperature, °R
$(t*\Delta P')$	Pressure derivative, psi
(t_D*P_D')	Dimensionless pressure derivative

Greek

Δ	Change
ϕ	Porosity, fracction
λ	Matrix-fracture network interporosity flow parameter
λ_f	Fracture network-Hydraulic fracture interporosity flow parameter
μ	Viscosity, cp
ξ	Variable to identify homogeneous (ξ=1) or heterogeneous ($\xi=\omega$) reservoirs
ω	Dimensionless storativity coefficient

Suffixes

$2BR$	Birradial flow in the homogenoeus región (second birradial)
$2BR$	Second birradial flow at the time of 1 hr
BR	Birradial
$BR1$	Birradial at 1 hr
$usBRi$	Intersect of birradial and unit-slope lines
D	Dimensionless
Dxf	Dimensionless based on half-fractured length
ell	Elliptical (same as birradial)
$L1$	Linear at 1 hr
$usLi$	Intersect of linear and unit-slope lines
max	Maximum point
min	Minimum point
w	Well
t	Time
us	Unit-slope during heterogeneous to homogeneous transition period
usi	Intersect of radial al unit-slope lines

REFERENCES

Agarwal G. 1979. Real Gas Pseudo-time a New Function for Pressure Buildup Analysis of MHF Gas Wells. Paper SPE 8279 presented at the 54th technical conference and exhibition of the Society of Petroleum Engineers of AIME held in Las Vegas, NV, September 23-26.

Cinco-Ley H., Samaniego F. and Dominguez N. 1976. Transient Pressure Behavior for a Well with a Finity-Conductivity Vertical Fracture. Paper SPE 6014 presented at the SPE-AIME 51st Annual Fall Technical Conference and Exhibition, held in New Orleans, LA, October 3-6.

Escobar F.H., Montealegre-M. M. and Martínez J.A. 2009. Conventional Pressure Analysis for Naturally Fractured Reservoirs with Transition Period before and After the Radial Flow Regime. CT and F - Ciencia, Tecnología y Futuro. 3(5): 85-106.

Escobar F.H., Ghisays-Ruiz A. and Bonilla L.F. 2014. New Model for Elliptical Flow Regime in Hydraulically-Fractured Vertical Wells in Homogeneous and Naturally-Fractured Systems. Journal of Engineering and Applied Sciences. ISSN 1819-6608. Vol. 9. Nro. 9: 1629-1636.

Martinez J.A., Escobar F.H. and Bonilla L.F. 2012. Reformulation of the Elliptical Flow Governing Equation for Horizontal Wells. Journal of Engineering and Applied Sciences. 7(3): 304-313.

Ozkan E. and Raghavan R. 1988, August 17. Some New Solutions to Solve Problems in Well Test Analysis: Part 2 - Computational Considerations and Applications. Society of Petroleum Engineers. doi:null

Tiab D. 1993. Analysis of Pressure and Pressure Derivative without Type-Curve Matching: 1- Skin and Wellbore Storage. Journal of Petroleum Science and Engineering. 12: 171-181.

Tiab D. 1994. Analysis of Pressure and Pressure Derivative without Type Curve Matching: Vertically Fractured Wells in Closed Systems. Journal of Petroleum Science and Engineering. 11: 323-333.

Tiab D. 2003. Advances in pressure transient analysis - TDS technique. Lecture Notes ManualThe University of Oklahoma, Norman, Oklahoma, USA. p. 577.

Tiab D. and Bettam Y. 2007. Practical Interpretation of Pressure Tests of Hydraulically Fractured Wells in a Naturally Fractured Reservoir. Society of Petroleum Engineers. doi:10.2118/107013-MS. January 1.

Appendix-A. Estimating half-fracture length by Conventional Analysis

Escobar et al. (2014) provided the following equation;

$$\Delta P = 9.4286\frac{q\mu B}{kh}\left(\frac{k}{\omega\phi\mu c_t x_f^2}\right)^{0.36} t^{0.36} \tag{A.1}$$

Or,

$$\Delta P = m_{ell} t^{0.36} \tag{A.2}$$

Which implies that a Cartesian plot of ΔP vs. $t^{0.36}$ (for drawdown) or ΔP vs. $[(t_p+\Delta t)^{0.36} - \Delta t^{0.36}]$ (for buildup) provides a straight line which slope, m_{ell}, provides the half-fracture length,

$$x_f = \sqrt{9.4286\frac{q\mu B}{khm_{ell}}\left(\frac{k}{\omega\phi\mu c_t}\right)^{0.36}} \tag{A.3}$$

During the homogeneous part, Equation (A.3) becomes:

$$x_f = \sqrt{9.4286\frac{q\mu B}{khm_{ell}}\left(\frac{k}{\phi\mu c_t}\right)^{0.36}} \tag{A.4}$$

If the early flow regime is linear, then:

$$\Delta P_{L1} = 4.064\left(\frac{qB}{h}\right)\sqrt{\frac{\mu t}{\phi c_t k\omega x_f^2}} \tag{A.5}$$

$$\Delta P_{L1} = m_L\sqrt{t} \tag{A.6}$$

So from the Cartesian plot of either pressure or pressure drop versus the square root of time:

$$x_f = 4.064\left(\frac{qB}{hm_L}\right)\sqrt{\frac{\mu}{\phi c_t k\omega}} \tag{A.7}$$

Appendix-B. Gas flow

Equations (1), (2) and (3) are applied to gas wells if the viscosity and total system compressibilities are given at initial conditions, it means $(\phi c_t)_i$. However, if those expressions are expressed using the pseudotime concept, Agarwal (1979), it yields:

ARPN Journal of Engineering and Applied Sciences

$$t_{Daxf} = \frac{0.000263kt}{\phi x_f^2} t_a(P) \tag{B.1}$$

For gas wells, Agarwal (1979) also included the pseudopressure definition,

$$m(P)_D = \frac{hk\left(m(P_i) - m(P)\right)}{1422.52 q_{sc} T} \tag{B.2}$$

which dimensionless pseudopressure derivative is given by:

$$t_D * m(P)_D' = \frac{hk\left(t * \Delta m(P)'\right)}{1422.52 q_{sc} T} \tag{B.3}$$

After replacing Equations (B.1), (B.2) and (B.3) into Equations (3) and (4) leads to obtain:

$$x_f = 529.16\left(\frac{q_{sc}T}{h(\Delta m(P)_{BR}}\right)^{1.3889} \sqrt{\frac{t_a(P)_{BR}}{\omega\phi k^{1.778}}} \tag{B.4}$$

$$x_f = 138.687\left(\frac{q_{sc}T}{h(t * \Delta m(P)'_{BR}}\right)^{1.3889} \sqrt{\frac{t_a(P)_{BR}}{\omega\phi k^{1.778}}} \tag{B.5}$$

$$x_f = 138.687\left(\frac{q_{sc}T}{h(t * \Delta m(P)'_{BR1}}\right)^{1.3889} \sqrt{\frac{1}{\omega\phi k^{1.778}}} \tag{B.6}$$

For the homogeneous zone:

$$x_f = 529.16\left(\frac{q_{sc}T}{h(\Delta m(P)_{2BR}}\right)^{1.3889} \sqrt{\frac{t_a(P)_{2BR}}{\phi k^{1.778}}} \tag{B.7}$$

$$x_f = 138.687\left(\frac{q_{sc}T}{h(t * \Delta m(P)'_{2BR}}\right)^{1.3889} \sqrt{\frac{t_a(P)_{2BR}}{\phi k^{1.778}}} \tag{B.8}$$

$$x_f = 138.687\left(\frac{q_{sc}T}{h(t * \Delta m(P)'_{2BR1}}\right)^{1.3889} \sqrt{\frac{1}{\phi k^{1.778}}} \tag{B.9}$$

In conventional analysis for gas flow case, Equation (3) becomes,

$$\Delta P = 94.989 \frac{q_{sc}T}{kh}\left(\frac{k}{\omega\phi x_f^2}\right)^{0.36} t_a(P)^{0.36} \tag{B.10}$$

20

Then, the slope of the Cartesian plot will give,

$$x_f = \sqrt{94.989 \frac{q_{sc}T}{khm_{ell}}\left(\frac{k}{\omega\phi}\right)^{0.36}} \tag{B.11}$$

For gas wells, Equations (13) and (14) become:

$$x_f = \frac{40.914\, q_{sc}T}{h(\Delta m(P))_{L1}}\left(\frac{1}{\omega\phi k}\right)^{0.5} \tag{B.12}$$

$$x_f = \frac{20.457\, q_{sc}T}{h\left(t * \Delta m(P)'\right)_{L1}}\left(\frac{1}{\omega\phi k}\right)^{0.5} \tag{B.13}$$

The analogous form of Equation (A.7) for gas flow is then:

$$x_f = \frac{40.914\, q_{sc}T}{hm_L}\left(\frac{1}{\omega\phi k}\right)^{0.5} \tag{B.14}$$

The gas version of Equations (20) to (23) is:

$$\lambda_f \approx 6560125.65\left[\frac{q_{sc}T}{kh[t * \Delta m(P')_{\max}]}\right]^{25/9} \tag{B.15}$$

$$\omega = \frac{\lambda_f k t_a(P)_{\max}}{1801.29\phi x_f^2} \tag{B.16}$$

$$\lambda_f = \frac{1801.29\omega\phi x_f^2}{k t_a(P)_{\max}} \tag{B.17}$$

Equation (24) for gas flow is:

$$\lambda_f = 20.463\left(\frac{\phi x_f^2 h[t * \Delta m(P')]_{us}}{q_{sc} B t_a(P)_{us}}\right)^{25/16} \tag{B.18}$$

Expressions (26) and (27) for gas wells:

$$\omega = 0.0002\left(\frac{t_a(P)_{\min}}{t_a(P)_{\max}}\right)^2 - 0.0155\left(\frac{t_a(P)_{\min}}{t_a(P)_{\max}}\right) + 0.2487 \tag{B.19}$$

Dividing Equation (B.6) by Equation (B.9) and solving for the storativity ratio:

$$\omega = \left[\frac{\left(t * \Delta m(P)'\right)_{2BR1}}{\left(t * \Delta m(P)'\right)_{BR1}}\right]^{2.7778} \tag{B.20}$$

ARPN Journal of Engineering and Applied Sciences

www.arpnjournals.com

Dividing Equation (B.13) by Equation (B.9) and solving for the storativity ratio:

$$\omega = 0.0218\left(\frac{h}{q_{sc}B}\right)^{0.778}\left[\frac{[t*\Delta m(P)']_{2BR1}^{1.3889}}{[t*\Delta m(P)']_{L1}}\right]^{2} k^{0.778} \quad \text{(B.21)}$$

Equations (29) and (31) rewritten for gas flow are:

$$\omega = \frac{1}{1456.69}\left(\frac{k\lambda_f t_a(P)_{usBRi}}{\phi x_f^2}\right)^{9/16} \quad \text{(B.22)}$$

$$\omega = \frac{6356.314\phi x_f^2}{k\lambda_f^{32/25} t_a(P)_{usLi}} \quad \text{(B.23)}$$

Finally, the gas versions for Equation (33) and (34) are:

$$\lambda_f = 345195361.5\left[\frac{q_{sc}T}{kh\Delta m(P)_{pss}}\right]^{25/9} \quad \text{(B.24)}$$

$$\omega = 0.3625\,\mathrm{e}^{-0.9877\frac{\Delta m(P)_{high}}{\Delta m(P)_{low}}} \quad \text{(B.25)}$$